

Searching for planetary transits and rotation periods in the Orion Nebula Cluster

Jonathan Irwin, Suzanne Aigrain, Simon Hodgkin, Mike Irwin
Institute of Astronomy, Cambridge, UK

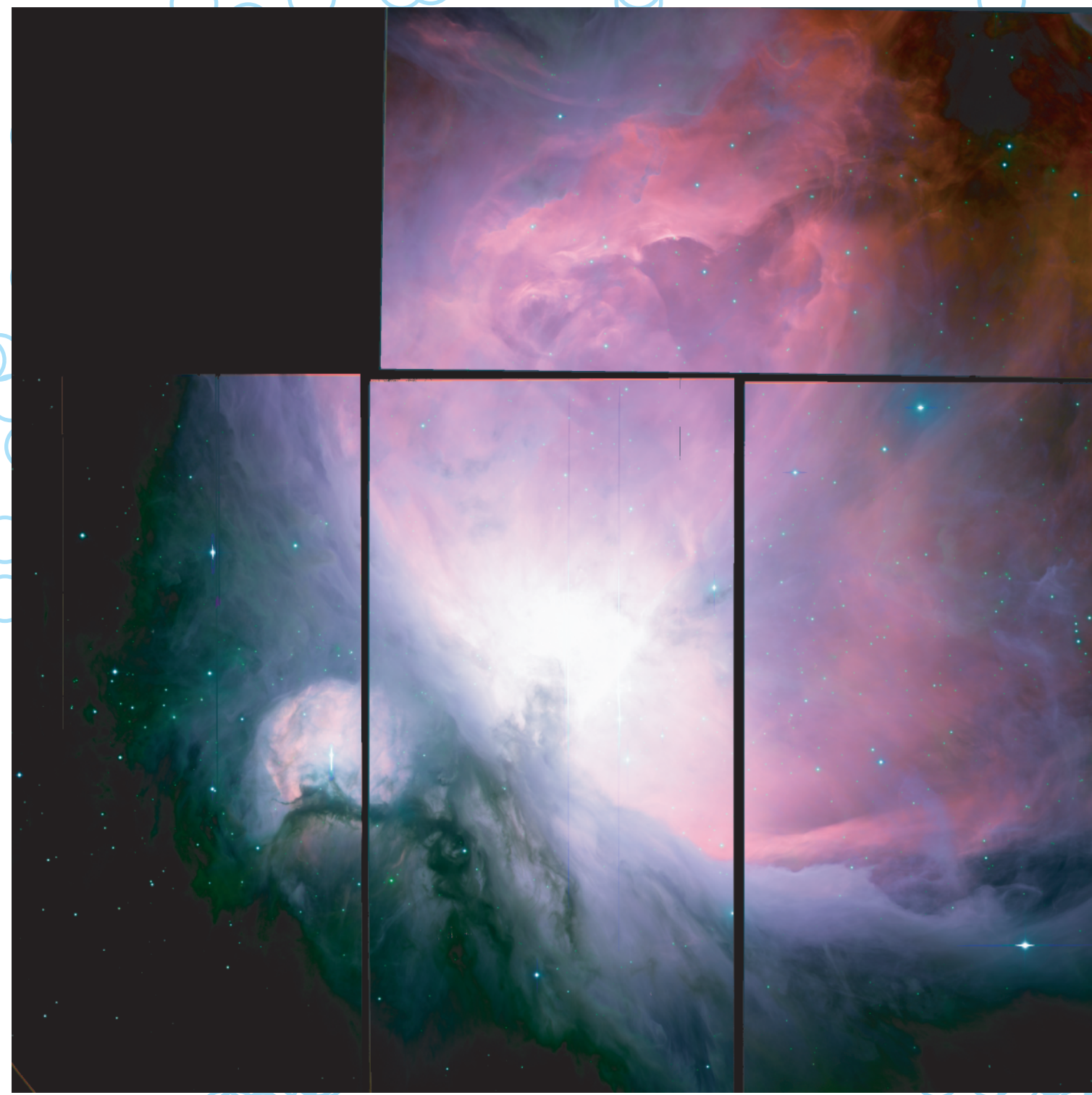


Figure 1: Colour image of the ONC region, generated from the INT photometric data taken in November 2004. The colours red, green and blue represent the H α , i and V bands respectively, with the overall intensity scaled by the H α image. North is to the left and East is down.

Introduction

We have undertaken a photometric monitoring campaign of the Orion Nebula Cluster (ONC) using the Isaac Newton Telescope (INT) Wide Field Camera (WFC) during November 2004. The primary goal of this survey is to search for transits by gaseous giant planets in close orbits around Pre-Main Sequence (PMS) stars.

Young stellar clusters provide an in-situ testing ground for planet formation scenarios. The detection of transiting planets around T Tauri stars (TTs) would provide important constraints for the planetary formation mechanisms, migration timescales and dynamical evolution, and their relation to disk lifetimes and clearing timescales (Bodenheimer & Lin 2002). The Orion Nebula Cluster's youth and richness makes it the ideal target for such a project (age 1 ± 1 Myr, >1600 PMS objects with and without disks with $l < 17.5$ in the central 0.2 sq.deg. Hillenbrand 1997).

While the present observations will enable us to search for planetary transits around primaries down to and beyond the brown dwarf limit (the photometric precision at $l=17$ being 1%), they are also suited to detecting eclipsing binary stars with at least one sub-stellar component. This would provide measures of the brown dwarf's luminosity, mass and radius and therefore constrain the mass-luminosity and mass-radius relations and their age dependency.

We also intend to study the rotational period distribution of the ONC members. Our observations, covering timescales from < 1 day to 1 month, and reaching substellar masses, will help determine at which stages disk locking is active, and how fast pre main sequence stars slow down onto the main sequence. Finally, optical short-term variability in TTs can be studied using our data for a large sample of objects, due to the high cadence we have obtained over the $\sim 34'$ field of view of the INT/WFC.

We completed the first INT observing run for this project at the end of November 2004. We present here the current status of the data analysis and outline some preliminary results.

Observations and data reduction

In November 2004, the ONC was typically observable from midnight onwards, and the first half of each night was used to observe the open cluster M34 (age 180 Myr).

For each cluster, alternate exposures of 30s in i' and 60s in V on a single pointing were taken continuously in alternance, resulting in an observing cadence of approximately 3 minutes 40 seconds. A small number of H α exposures (typically 2 per night) were also taken, using exposure times of 100s in the ONC (chosen to avoid saturating the nebulosity) and 300s in M34. Figures 1 and 2 show colour images of the two regions, generated from the INT data. During the run a total of 280 V and i' pairs of frames for M34 and 377 for the ONC were obtained over 10 nights.

The INT data were reduced using the standard INT Wide Field Survey (WFS) pipeline (Irwin & Lewis 2001), including crosstalk correction, bias correction, flatfielding, defringing (for the i' data), astrometric calibration and photometric calibration using observations of Landolt (1992) standard star fields. For the ONC data it was necessary to modify the standard astrometric routines to use the 2MASS point source catalogue since there was insufficient coverage in the USNO and APM catalogues due to the bright nebulosity in the region.

Analysis and preliminary results

Due to the presence of extensive nebulosity in the ONC region, it was necessary to use Difference Image Analysis (DIA) to perform the photometry. Our initial experiments concentrated on the M34 data, since this was much more straightforward to analyse and could be used to compare results from our standard aperture photometry software with those from the DIA routines written specifically for this project.

Aperture photometry

We first analysed the M34 data using standard pipeline aperture photometry routines. Briefly, the procedure consisted of generating a master catalogue from a stacked image of 20 frames taken in good seeing and sky conditions (parameterised by a low sky RMS, corresponding to low lunar illumination and no cloud). A total of 13700 objects were included in the master catalogue, approximately uniformly distributed across all four detectors.

The master catalogue was then used as a reference frame to refine the astrometric solutions of all the individual data frames. This procedure reduces the differential astrometric error between frames to negligible levels and minimises photometric errors resulting from slightly different placement of apertures between frames.

The resulting frames were used to perform aperture photometry in the usual way, using the master catalogue as a reference. We applied a 2-D polynomial fit correction to the lightcurve residuals as a function of position on each CCD to remove any temporally- and spatially-varying residuals. The resulting plot of the RMS scatter of each object as a function of magnitude is shown in Figure 3 (right).

Difference image analysis

The input frames for the aperture photometry (see above) were used to perform a DIA version of the M34 photometry using an adaptive kernel technique (Alard & Lupton 1998, Alard 2000), with the master frame used as a reference image. Standard aperture analysis was then performed on the difference images, using the same master catalogue. The resulting RMS plot is shown in Figure 3 (above right) and shows a small improvement in the number of outliers.

The DIA technique is also illustrated in Figure 4 (right), which shows images from the ONC region. The adaptive kernel image subtraction technique takes account of the difference in the image PSF (due to, for example, varying seeing) between the two frames to be subtracted and we have also included an option to remove any slowly (spatially) varying differential background component.

The use of these image subtraction techniques largely eliminates residuals in the subtracted images due to PSF variations between the frames, and is the only viable method for the ONC region.

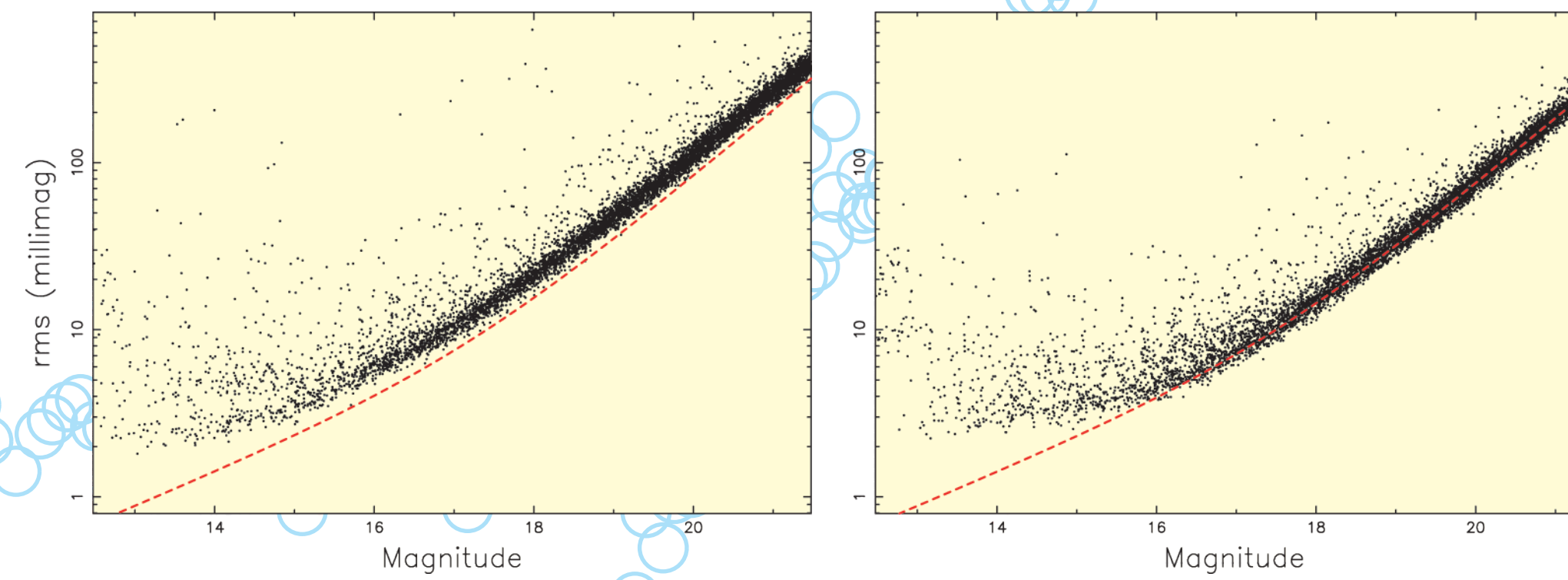


Figure 3: Plots of the RMS scatter as a function of magnitude for all objects in the M34 field classified as stellar, using our standard aperture photometry (left) and difference image analysis using an adaptive kernel technique (right), for the November 2004 data. The dashed line shows the expected RMS, calculated as the quadrature sum of contributions from the readout noise, sky noise in the photometric aperture and the photon noise.

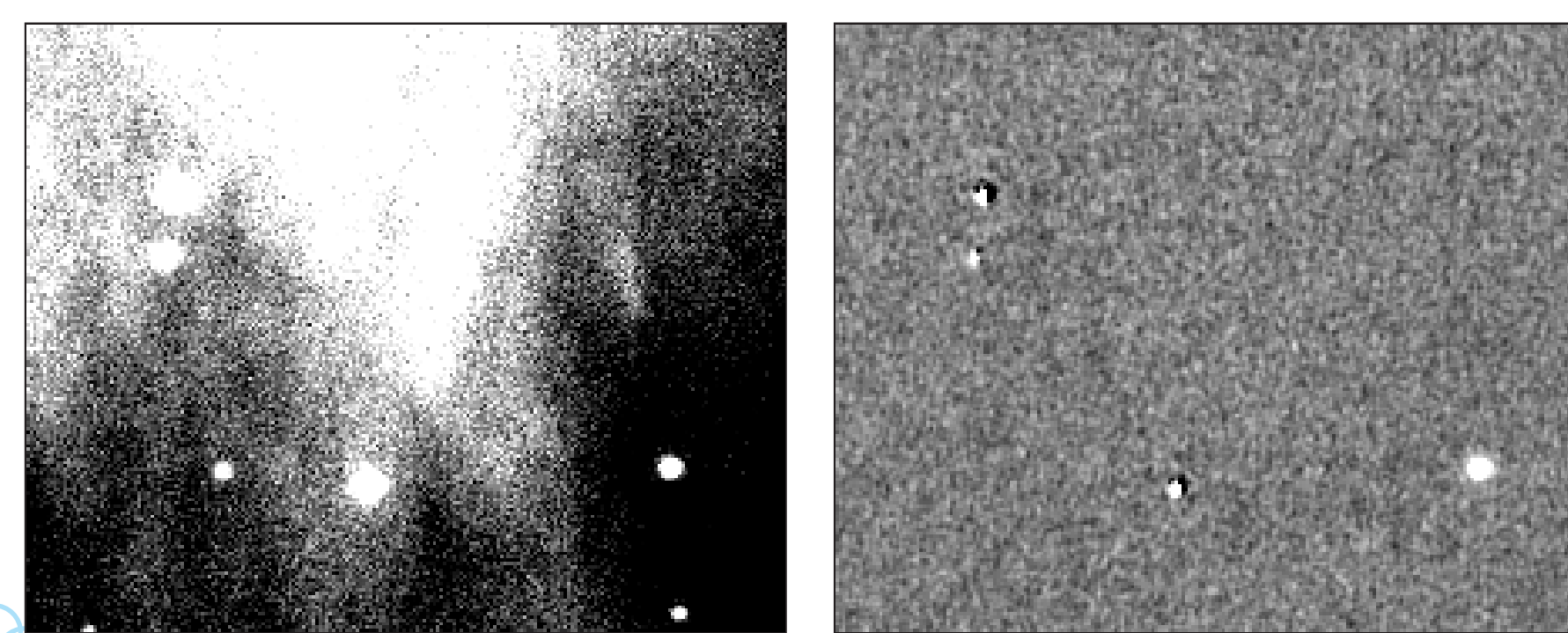
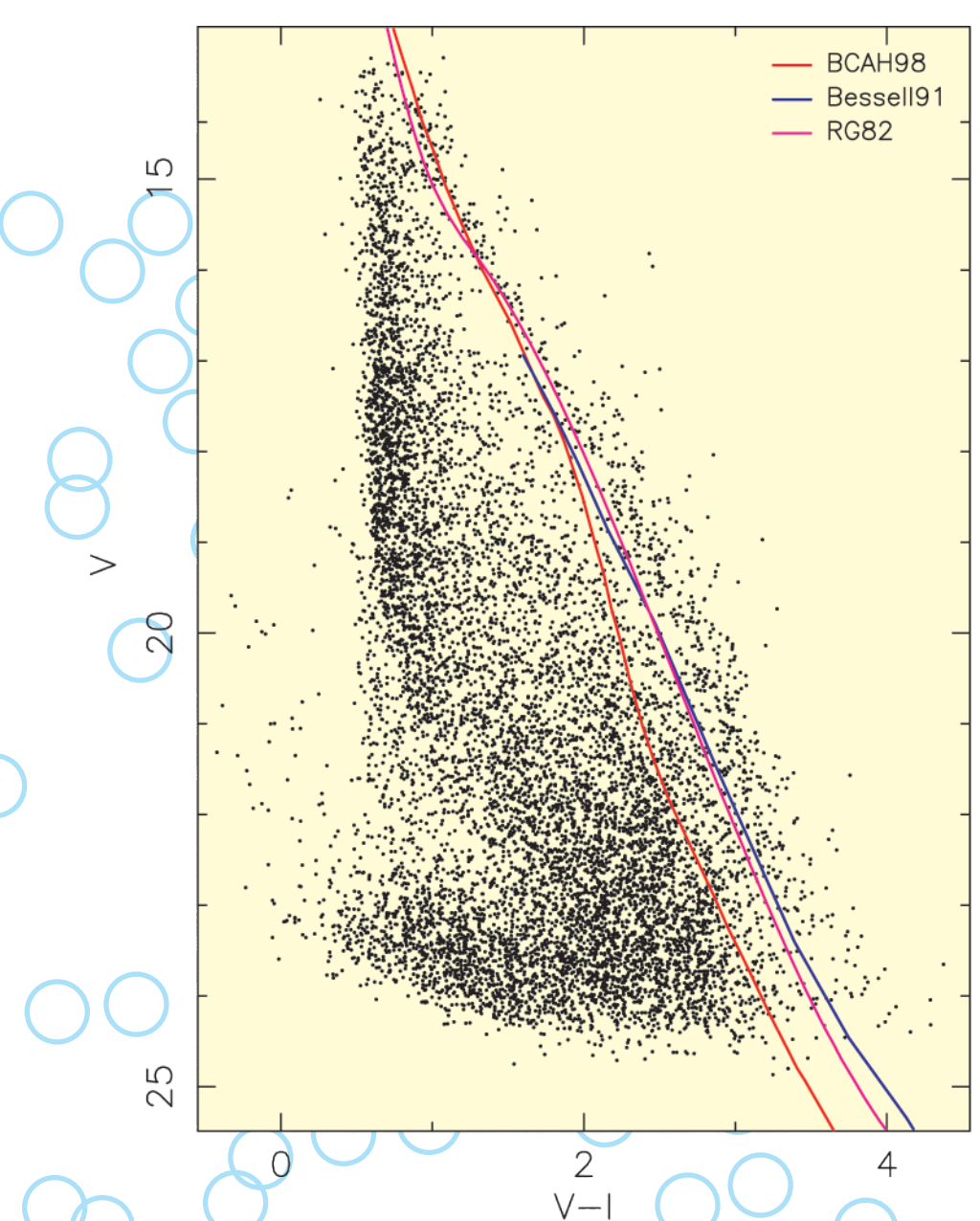


Figure 4: Sample section from an i' frame of the ONC on CCD 4, close to the central bright region of the nebula (left) and the corresponding difference image (right), illustrating the very effective removal of the nebula. These images are linearly scaled, with black corresponding to the sky level - 7s and white to the sky level + 7s (where s is the sky level on the difference image), and show approximately 225x180 pixels. The star at the right of the images has varied with respect to the master frame.



Colour-magnitude diagrams

A colour magnitude diagram for M34 was generated by stacking 120x60s V and 30s i' band images from the same data-set used for the photometry. The resulting plot is shown in Figure 5 (left). The cluster sequence is clearly visible to the right-hand side of the diagram.

Figure 5: V against V-I colour magnitude diagram for the M34 data. The diagram was generated from stacks of 120x 60s V and 30s i' band images respectively, all taken at low airmass, on photometric nights with good seeing conditions. The limiting magnitudes for 5- σ detections were approximately 24.5 in V and 23.3 in i'. The CCD magnitudes were converted to the standard Johnson-Cousins system of Landolt (1992) using colour equations taken from the INT wide field survey web pages. The red line shows the 160 Myr isochrone of Baraffe et al. (1998) at the assumed distance modulus of 8.7 and reddening of $E(B-V) = 0.07$ taken from the WEBDA database. The blue line shows the results for old disk M-dwarfs from Bessell (1991), and the magenta line shows the empirical fiducial main sequence for the solar neighbourhood of Reid & Gilmore (1982).

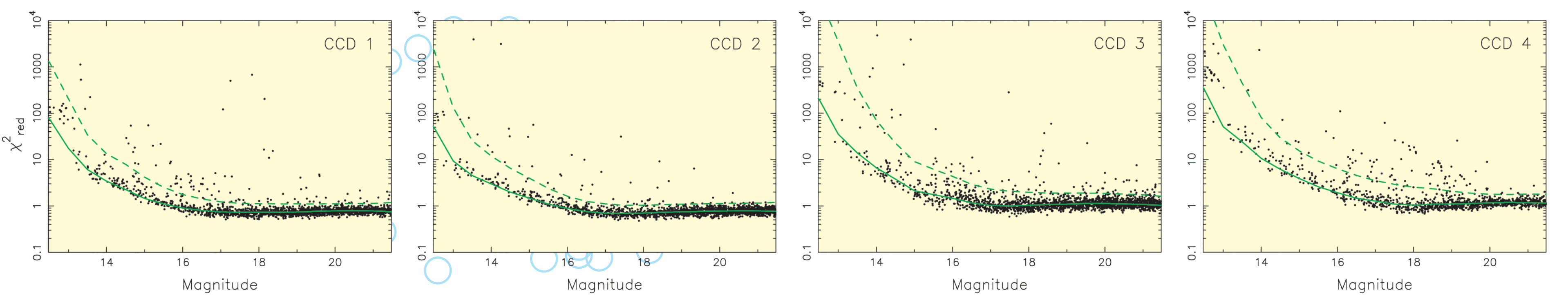


Figure 6: Plots of the reduced χ^2 statistic for all objects classified as stellar on each CCD, calculated using an estimate of the random noise in the photometric aperture for each object (not including systematics, hence the turn-up at bright magnitudes). The overlaid solid line shows the median calculated in 0.5 mag bins, smoothed by a 1-2-1 Hanning filter, and the dashed line shows the median + 3 σ (using a robust MAD estimator) also smoothed by a 1-2-1 Hanning filter. All objects above the dashed line were selected as candidate variables.

Searching for variable objects

The lightcurves generated from the M34 difference image analysis were used in a variable star search. A simple technique, using the reduced χ^2 of the lightcurves, was adopted as an initial test. The selection criteria for variable objects are detailed in Figure 6 (above right), with some example lightcurves, probably contact binary systems, selected using this technique in Figures 7 and 8 (below and right).

A large number of variable objects were seen in the ONC displaying a variety of behaviour. Some example lightcurves for this region are shown in the remaining Figures 9-11 (right and below right), displayed over the entire November 2004 data-set.

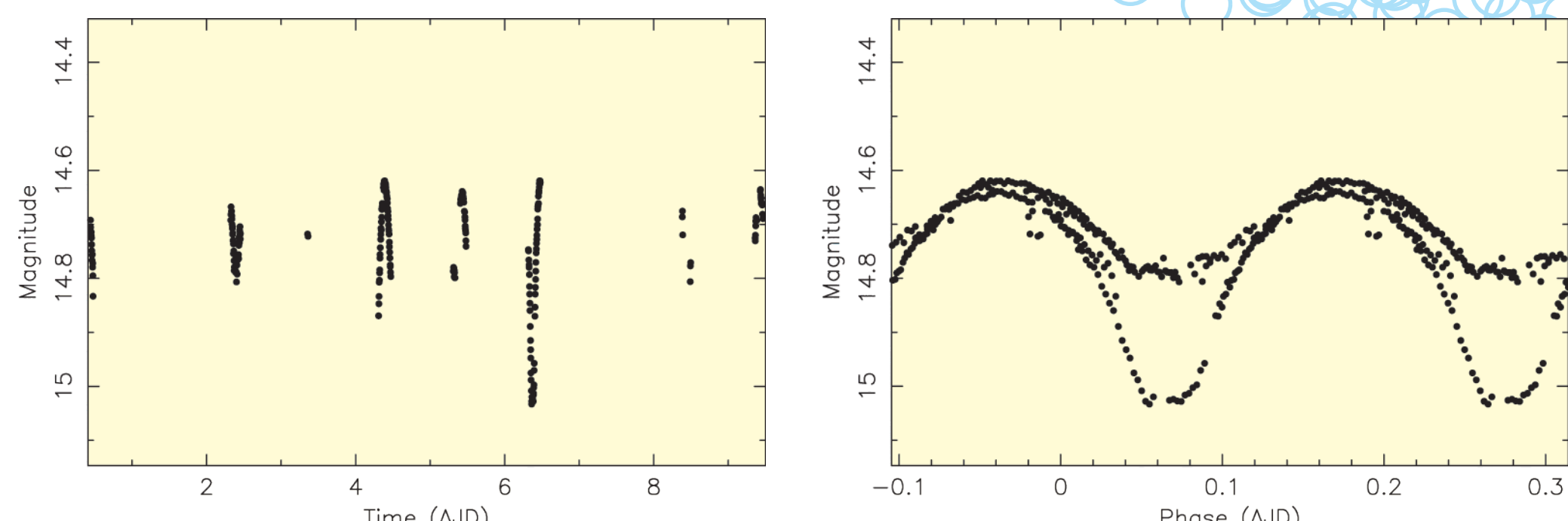


Figure 7: Original (left) and phase-folded (right) i'-band lightcurves for a candidate eclipsing binary on CCD #3 of the M34 data. The determined period is 0.209 days (used for the phase-folded lightcurve plot), or 0.418 days assuming the apparent secondary eclipses are real. This object has an i' magnitude of 14.75 and an amplitude of 0.108 mag, with a V-I colour of 0.392. The time axes are plotted in differential Julian days, measured with respect to the first data point at MJD = 53326.443.

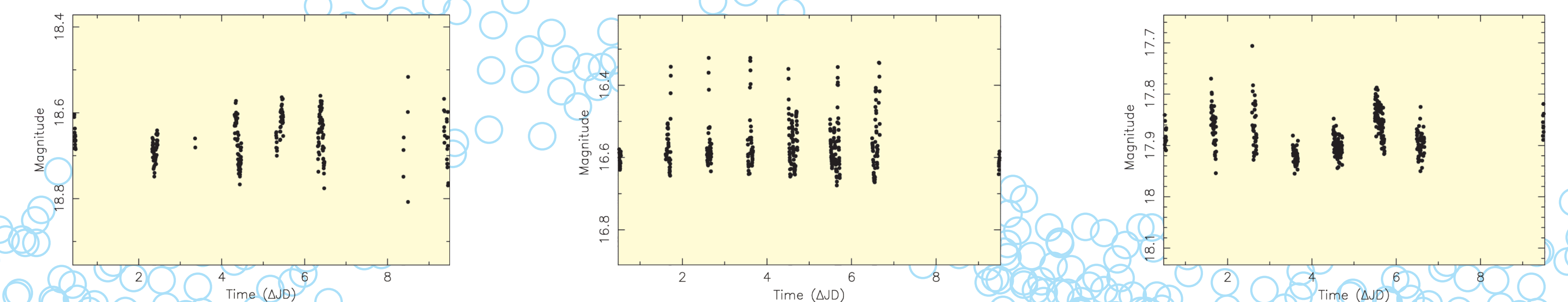


Figure 8: Original (top) and phase-folded (bottom) i'-band lightcurves for a candidate periodic variable star on CCD #2 of the M34 data. The determined period is 0.187 days. This object has an i' magnitude of 18.66 and an amplitude of 0.062 mag, with a V-I colour of 0.388.

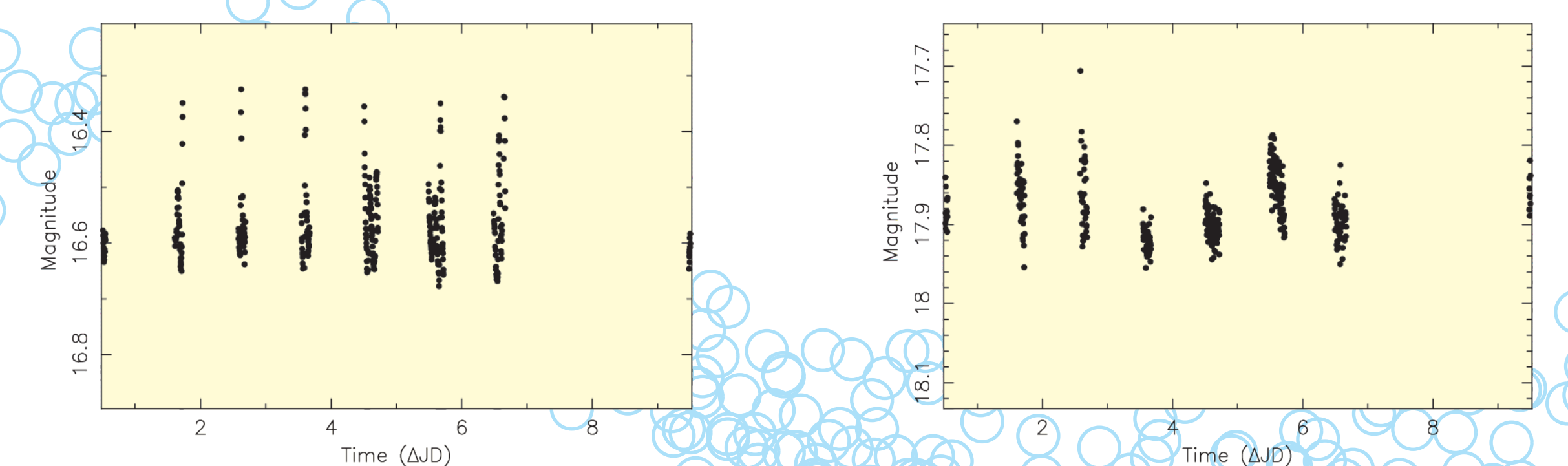


Figure 9: Original (top) and phase-folded (bottom) i'-band lightcurves for a candidate periodic variable object on CCD #3 of the ONC data. The phase-folded lightcurve used a period of 0.09 days, the interval between the peaks. This object has an i' magnitude of approximately 16.6 and an amplitude of 0.1 mag. The time axes are plotted in differential Julian days, measured with respect to the first data point at MJD = 53326.508.

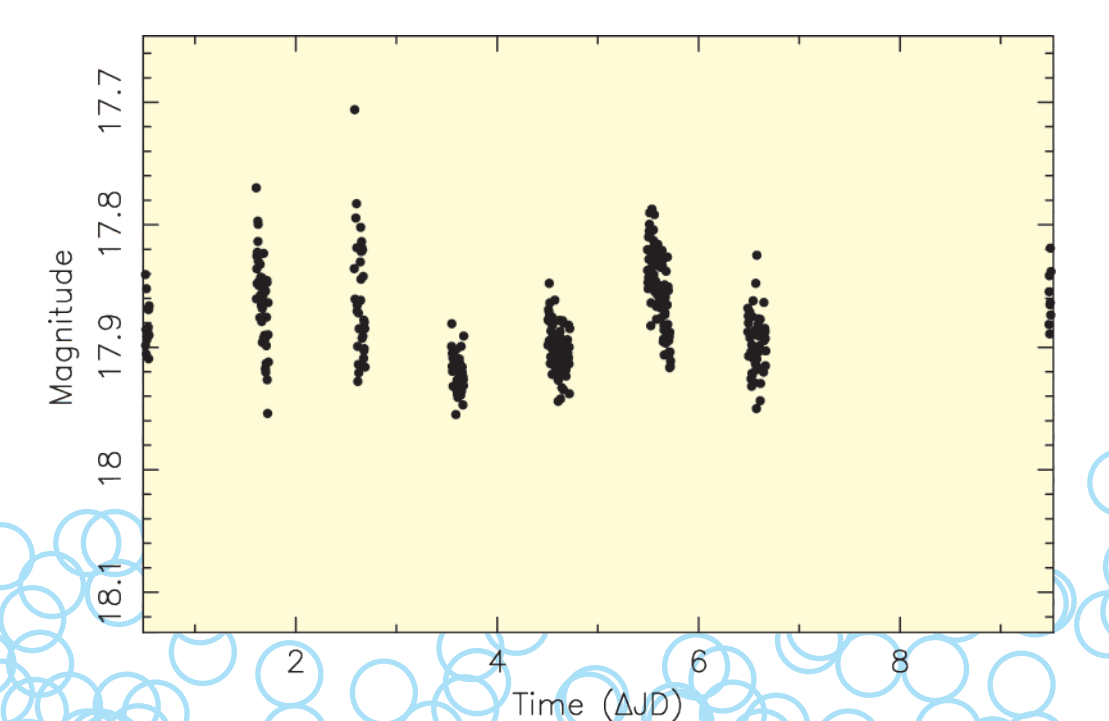


Figure 10: Original (top) and phase-folded (bottom) i'-band lightcurves for a candidate periodic variable object on CCD #4 of the ONC data. The determined period is 0.574 days. This object has an i' magnitude of approximately 17.9 and an amplitude of 0.04 mag.

Conclusions and future work

We have performed photometry on the November 2004 data of M34 using both standard aperture photometry and DIA. Examination of the lightcurves (eg. Figures 7 and 8) and RMS plots (Figure 3) for the M34 data indicate that the DIA technique works well on INT data. The ONC data have thus been analysed only using DIA. Generating the master catalogue proved somewhat problematic. We are currently using a combined 2MASS and colour-magnitude diagrams, 1998 A&A 337, 403 by matching our optical source positions against those objects in the 2MASS point source catalogue in the ONC region with detections in the J and K bands. This yielded a total of 1787 objects over our $34'$ field of view. Some commissioning data from the UKIRT WFCAM instrument in this region may become available soon and we will investigate using this as a deeper substitute for the 2MASS data. A second (January 2005) INT observing run is currently underway at the time of writing, and will provide further ONC observations.

The analysis of the M34 and ONC data is still underway. We will continue the process of searching for variable stars and periodicities, and will investigate automatic methods for their classification. We will compare the rotation periods we measure to those derived in X-rays from the Chandra Orion Ultra-deep Project (COUP, PI Feigelson).

We will also search the light curves for transit-like events. Both star and planet are bloated in the T Tauri phase (Rhode et al. 2001, Bodenheimer et al. 2001), which leads to enhanced transit probabilities, but transit depths similar to those observed in older systems. The intrinsic variability of PMS stars (our preliminary lightcurves show variability at the few percent level for the vast majority of the ONC objects) constitutes an interesting but not insurmountable challenge for transit detection, particularly for non-accreting stars, whose variations are often dominated by a periodic rotational modulation component. We will use the transit search algorithm and variability filters developed in Aigrain & Irwin (2004), which we will adapt to the specificities of the present project. In particular, tidal synchronisation implies a likely common period between any rotational and planetary signals which can be exploited to maximise the detection performance.

The present observations are part of the Monitor project, a large collaboration to search for transits and substellar eclipsing binaries in young open clusters, which has been allocated time in 2005A on CFHT+MegaPrime, CTIO+Mosaic and ESO2.2m+WFI to perform a similar analysis on IC4665, Blanco 1, NGC2362 and M50.

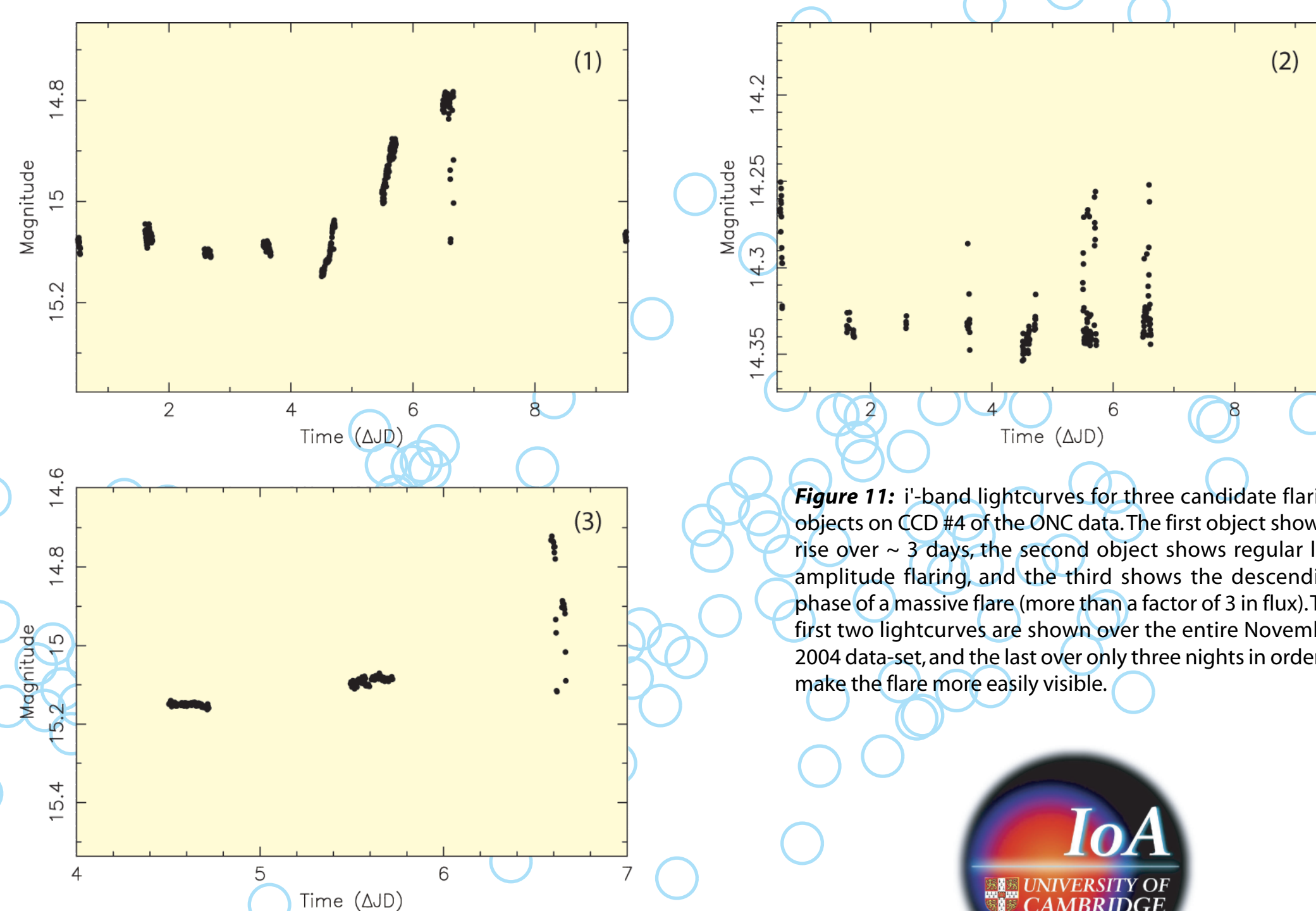


Figure 11: i'-band lightcurves for three candidate flaring objects on CCD #4 of the ONC data. The first object shows a rise over ~ 3 days, the second object shows regular low-amplitude flaring, and the third shows the descending phase of a massive flare (more than a factor of 3 in flux). The first two lightcurves are shown over the entire November 2004 data-set, and the last over only three nights in order to make the flare more easily visible.

References

1. Aigrain & Irwin, Practical planet prospecting, 2004 MNRAS 350, 331
2. Alard & Lupton, A Method for Optimal Image Subtraction, 1998 ApJ 503, 325
3. Alard, Image subtraction using a space-varying kernel, 2000 A&AS 114, 363
4. Baraffe, Chabrier, Allard & Hauschildt, Evolutionary models for solar metallicity low-mass stars: mass-magnitude relationships and color-magnitude diagrams, 1998 A&A 337, 403
5. Bessell, The late-M dwarfs, 1991 AJ 101, 662
6. Bodenheimer, Lin & Marling, On the Tidal Inflation of Short-Period Extrasolar Planets, 2001 ApJ 548, 466
7. Bodenheimer & Lin, Implications of Extrasolar Planets for Understanding Planet Formation, 2002 AREPS 30, 113
8. Herbst, Nailer-Jones, Mundi, et al., Stellar rotation and variability in the Orion Nebula Cluster, 2002 A&A 396, 513
9. Hillenbrand, On the Stellar Population and Star-Forming History of the Orion Nebula Cluster, 1997 AJ 113, 1733
10. Irwin & Lewis, INT WFS pipeline processing, 2001 NewAR 45, 105
11. Landolt, UBVR photometric standard stars in the magnitude range 11.5-16.0 around the celestial equator, 1992 AJ 104, 340
12. Rhode, Herbst & Mathieu, Rotational Velocities and Radii of Pre-Main-Sequence Stars in the Orion Nebula Cluster, 2001 AJ 122, 3258
13. Reid & Gilmore, New light on faint stars. II - A photometric study of the low luminosity main sequence, 1982 MNRAS 201, 73

